Pis'ma v ZhETF, vol. 93, iss. 3, pp. 154 – 158 © 2011 February 10

The low-temperature macroscopic phase separation in $La_{0.5}Ba_{0.5}CoO_{3-\delta}$ cobaltite

I. O. Troyanchuk[◇1)], *D. V. Karpinsky*[◇], *M. V. Bushinsky*[◇], *V. Sikolenko*[○⋆], *V. Efimov*[⋆], *A. Cervellino*[▽]

[◇] *SSPA "Scientific-Practical Materials Research Centre of NAS of Belarus", 220072 Minsk, Belarus*

[○] *Laboratory for Neutron Scattering, ETH Zurich and Paul Sherrer Institute, CH-5232 Villigen, Switzerland*

[⋆] *Joint Institute for Nuclear Research, Dubna, RU-141980 Russia*

[▽] *Swiss Light Source, Paul Sherrer Institute, CH-5232 Villigen, Switzerland*

Submitted 8 December 2010

$La_{0.5}Ba_{0.5}CoO_{2.87}$ has been characterized with neutron and synchrotron powder diffraction and magnetization measurements. This compound was shown to have a cubic crystal structure at temperatures above 200 K whereas slightly above the Curie point $T_c \sim 170$ K the structural separation into two different pseudocubic phases gradually develops upon cooling. The structural transformation is reversible. At 2 K the sample consists of G-type antiferromagnetic oxygen-poor and ferromagnetic oxygen-rich phases (approximately 33% and 66% respectively).

Rare earth cobaltites with an $LnCoO_3$ perovskite structure and hole-doped $Ln_{1-x}A_xCoO_3$ (Ln = lanthanide, A = alkaline earth metal: Ca, Sr or Ba) attract much interest as they exhibit a variety of unusual magnetic and transport properties [1–5]. The Co ions in an octahedral symmetry may have either a high, intermediate or low-spin state as the energies of the crystal-field splitting of both the Co *3d* states E_{cf}) and the Hund's rule exchange energy (E_{ex}) are comparable. In the ground state at low temperature, $LaCoO_3$ contains Co^{3+} ions with the low-spin electronic configuration $t_{2g}^6e_g^0$. Upon heating, the spin state of Co ions thermally activates to an intermediate state (IS, $t_{2g}^5e_g^1$, $S = 1$) or high-spin state (HS, $t_{2g}^4e_g^2$, $S = 2$). However the spin transition is incomplete up to 500 K, where insulator-metal transition takes place [1].

In the hole-doped cobaltites, $La_{1-x}A_xCoO_3$, the additional Co^{4+} ion increases the complexity of the system as it can also appear with a variety of spin states. Among doped cobaltites, the system $La_{1-x}Sr_xCoO_3$ is the most extensively investigated. A spin glass behavior was reported for $0.01 < x < 0.18$ as well as a ferromagnetic long-range ordering that coincides with concentration insulator-to-metal transition for $x > 0.18$ [6]. Similar metallic ferromagnetic state was observed in barium-doped cobaltites with the barium content $x > 0.2$ [7–9]. The nature of the ferromagnetic state in cobaltites has been a subject of debates for a long time [10–12]. Three main mechanisms were suggested for magnetic properties of mixed-valence cobaltites: the superexchange model based on the localized electron interaction via oxygen ion, the Zener double exchange via charge transfer and the itinerant electron ferromagnetism [10–12].

The structural studies performed on the cubic oxygen-stoichiometric perovskite $La_{0.5}Ba_{0.5}CoO_3$ have revealed the onset of a long-range tetragonal phase accompanying a para-ferromagnetic transition occurring at $T_C = 180$ K [13]. The tetragonal distortion has been discussed in terms of cooperative and static Jahn-Teller distortions of the CoO_6 octahedra. It was assumed that the Jahn-Teller effect is favored by the intermediate spin-state configuration, of the $Co^{3+}(d^6)$ and $Co^{4+}(d^5)$ ions derived from the measured ferromagnetic moment -1.9 μ_B per cobalt ion. However, the Sr-doped ferromagnetic cobaltites have approximately the same magnetic moment value and do not exhibit a structural transition at the Curie point [14, 15]. Moreover the extended X-ray absorption fine structure (EXAFS) and neutron diffraction studies do not reveal an appreciable local Jahn-Teller distortion in $La_{1-x}Sr_xCoO_3$ [16].

Beside the alkaline earth doping there is another way to manipulate the physical properties of the rare earth cobaltites. It was shown that the oxygen content in the Ln and Ba ordered perovskite systems $LnBaCo_2O_y$ can be varied in a wide range from $y = 4.5$ to $y = 6$ that leads to a change of the average oxidation state of the cobalt ions from 2+ to 3.5+ [17–19]. The intermediate $LnBaCo_2O_{5.5}$ phase shows very interesting properties, such as metal-insulator transition, antiferromagnetic-ferromagnetic transition and the giant magnetoresistance effect [17–19]. The Curie point of $LaBaCo_2O_{5.5}$ is the largest and reaches 326 K [20]. The reduction of

[1)] e-mail: troyan@physics.by

the oxygen content from $y = 3$ down to $y = 2.25$ has been reported for $La_{0.5}Sr_{0.5}CoO_y$ perovskite [21]. This oxygen content corresponds to nominal Co^{2+} oxidative state. Considering these reports we have decided to investigate the effect of oxygen deficiency on structural and magnetic properties of $La_{0.5}Ba_{0.5}CoO_{3-y}$ cobaltite. In this paper we report on macroscopic reversible structural phase separation into two different pseudocubic antiferromagnetic and ferromagnetic phases. Oxygen migration is involved into the phase separation mechanism.

Ceramic samples of $La_{0.5}Ba_{0.5}CoO_{3-\delta}$ compositions were prepared by a solid-state phase reaction method using high-purity $BaCO_3$, La_2O_3 and CoO taken in stoichiometric ratio and thoroughly mixed with a planetary ball mill (RETSCH PM-100). The synthesis was performed at 1200 °C for 10 hours in air, followed by cooling at rate of 300 °C/h down to 400 °C. Synchrotron powder diffraction (SPD) experiments were carried out at the Swiss Light Source synchrotron of the Paul Scherrer Institute using MS beamline (wavelength 0.49 Å). The neutron powder diffraction (NPD) experiments were performed using a high-resolution diffractometer E9 at the Berlin Neutron Scattering Center (BENSC) of Helmholtz-Zentrum Berlin (HZB). The neutron and X-ray powder diffraction data were analyzed using the Rietveld method incorporated into the FullProf software package [22]. Magnetic properties were studied with a SQUID-magnetometer (MPMS-5, Quantum Design).

Figure 1a presents the temperature dependence of the magnetization of the $La_{0.5}Ba_{0.5}CoO_{3-\delta}$ sample. Both field-cooled (FC) and zero field-cooled (ZFC) data are presented: the field cooling was performed in a magnetic field of 100 Oe. In the temperature range of 160–170 K the $M(T)$ dependencies exhibit a sharp drop in both the FC and ZFC magnetization confirming a transition into paramagnetic state. The temperature onset of the magnetic ordering ($T_C \sim 170$ K) is slightly lower than in stoichiometric $La_{0.5}Ba_{0.5}CoO_3$ in which the ferromagnetic-paramagnetic transition occurs near $T_C \sim 180$ K [13]. The ZFC magnetization has a nonmonotonic behavior with a peak close to the temperature at which FC magnetization starts to decrease. In the cobaltites the magnetization curve in low external field is governed by an anisotropy field [23] so the large difference between ZFC and FC may result from a large magnetic anisotropy which enhances strongly at low temperature. The $M(H)$ curves measured in magnetic fields up to 50 kOe at different temperatures (Fig.1b) show a monotonic increase in magnetization as temperature decreases. The estimated magnetic moment per Co ion is close to $1.1\,\mu_B$ at liquid helium temperature. This

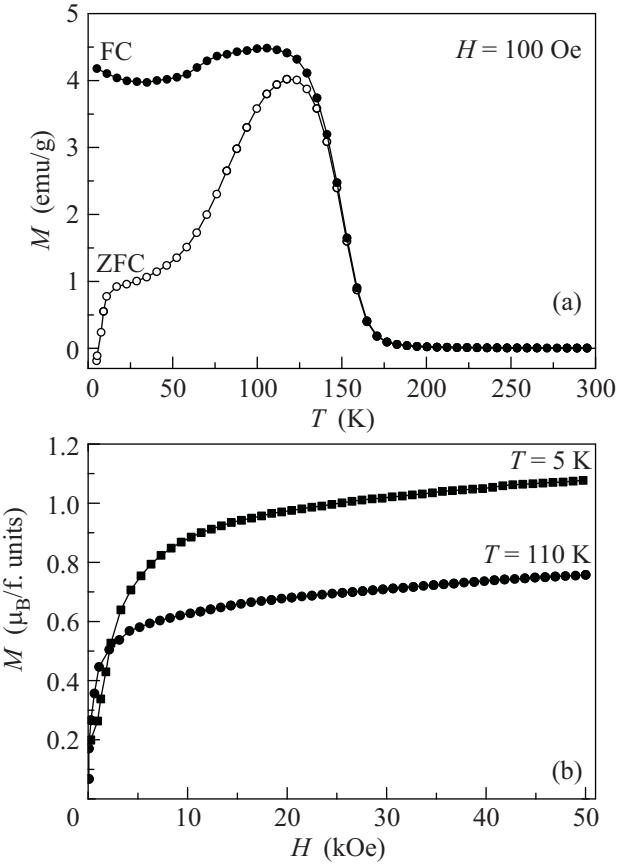

Fig.1. Temperature dependences of the dc magnetization in a field of 100 Oe for $La_{0.5}Ba_{0.5}CoO_{2.87}$. (a) ZFC curves are shown as open symbols, whereas FC curves are shown as solid symbols; (b) Magnetization vs. magnetic field dependences

value is much lower compared with $1.9\,\mu_B$/Co reported for stoichiometric $La_{0.5}Ba_{0.5}CoO_3$ [13].

NPD patterns of $La_{0.5}Ba_{0.5}CoO_{3-\delta}$ were recorded at room temperature, 150, 120, 80 and 2 K, and for clarity only two of them are displayed in Fig.2. The first pattern recorded at 300 K is characteristic of the high-temperature structural state which extends down to $\sim$ 200 K as follows from the SPD study. At room temperature the Rietveld refinement leads to a simple cubic cell $a_p \times a_p \times a_p$ with the space group $Pm\bar{3}m$ (global $\chi^2 = 1.76$). The observed, calculated and difference patterns of this sample recorded at 300 K are displayed in Fig.2. Alternatively, the experimental pattern can be refined using tetragonal space group $P4/mmm$; rhombohedral space group $R\bar{3}c$ or orthorhombic $Pnma$ but without significant increase in the quality of the fit. Thus, according to the Rietveld refinement we keep the model with the highest symmetry. The refined value of the oxygen content is 2.87 which is significantly below the stoichiometric value. The $Pm\bar{3}m$ crystallographic

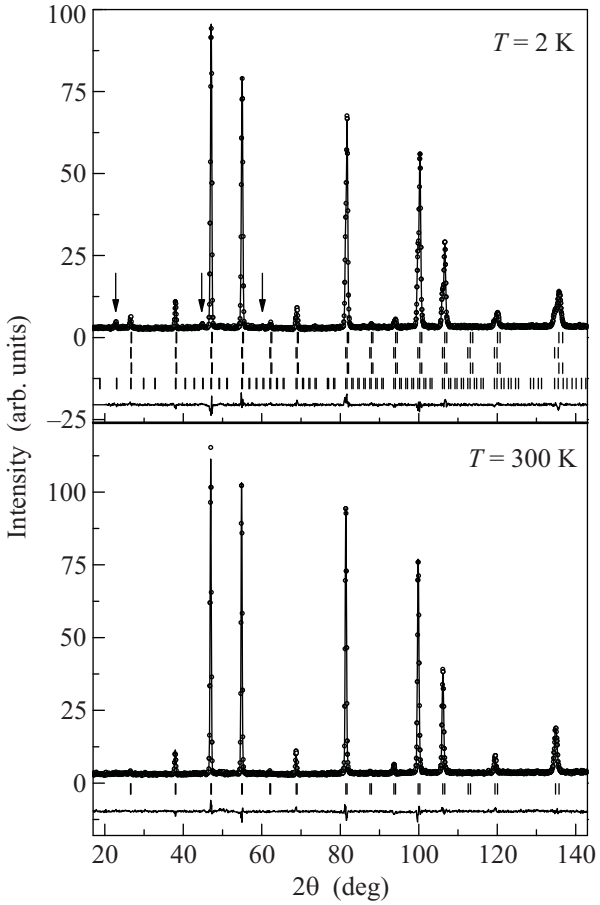

Fig.2. Neutron powder diffraction data collected from $La_{0.5}Ba_{0.5}CoO_{2.87}$ at 2 and 300 K. Solid arrows mark diffraction peaks due to simple G-type antiferromagnetic order. The points and the line refer to measurements and calculation including ferromagnetic and antiferromagnetic contributions, the bottom line represents their difference. Data are refined in space group $Pm\bar{3}m$ for both structural phases

structure means that both La and Ba ions as well as oxygen vacancies are distributed statistically over lattice. At 150 K we have noticed an asymmetric broadening of all the peaks which develops strongly upon cooling to 120 K. For the patterns recorded at 80 and 2 K we clearly observed a splitting of all the peaks at $2\theta > 60°$ and an appearance of new small peaks strongly separated from the basic peaks described with $Pm\bar{3}m$ space group.

SPD experiments were performed in order to clarify a reason for NPD peaks splitting and appearance of the new peaks. The SPD spectra were recorded at every 5 K from 4 K up to room temperature using the same sample as for the NPD study. Parts of the selected spectra are presented in Fig.3 which reveals that the sample in the low-temperature state consists of two phases with

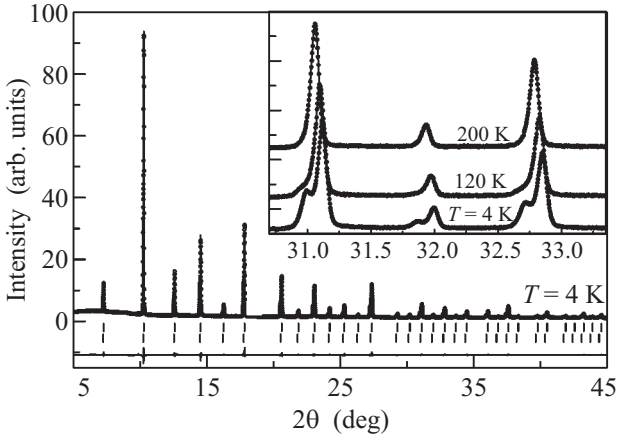

Fig.3. Synchrotron diffraction patterns of $La_{0.5}Ba_{0.5}CoO_{2.87}$. The points and the line refer to measurements and calculation; the bottom line represents their difference. Data are refined in space group $Pm\bar{3}m$ for both structural phases. The inset shows the magnified parts of the patterns at selected temperatures

different parameters of the unit cell. The volume ratio between the two phases at 2 K is approximately 1:2 where the major phase is closer to the high-temperature structural state. The amount of the minor phase, which has a larger unit cell decreases gradually upon warming up, and disappears completely above 200 K where the sample consists of one cubic phase. In contrast with NPD study we did not observe additional diffraction peaks associated with deviation from cubic symmetry of both low temperature phases, suggesting that additional peaks observed at low temperature in NPD patterns result from magnetic ordering. We suggest that both phases have a cubic unit cell at low temperature which can be described with $Pm\bar{3}m$ space group. The Rietveld refinement in this model gave a satisfactory fit for the SPD pattern recorded at 4 K (Fig.3). The temperature behavior of the cubic unit cell parameters for both phases is presented in Fig.4. In the temperature range where two phases coexist the unit cell parameters of both phases slightly increase with temperature. There is no evidence for intermediate state between phases with close unit cell parameters.

The Rietveld refinement of the NPD spectra acquired at 2 K in the two cubic phase model leads to satisfactory description of basic structural peaks for both the structural phases. The fit was further improved by taking into account magnetic neutron scattering. The additional peaks appearing at low temperature can be well indexed in $2a_p \times 2a_p \times 2a_p$ supercell where a_p is unit cell parameter for the minor phase with larger unit cell parameter. This means that the magnetic structure associated with the minor phase is G-type antiferromag-

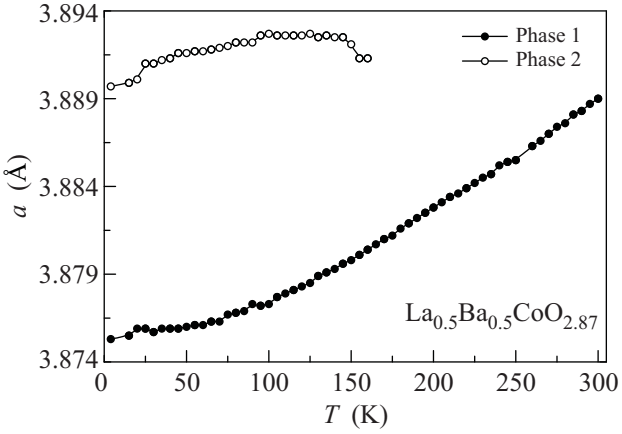

Fig.4. Temperature dependence of the unit cell parameters for $La_{0.5}Ba_{0.5}CoO_{2.87}$

netic. The calculated magnetic moment for this phase is $\pm 2.1\mu_B$/Co. The major phase is ferromagnetic with magnetic moment about $1.6\mu_B$/Co. The oxygen content of the minor phase was roughly estimated as 2.75 whereas for the major phase it was close to 2.92 from Rietveld refinement of 2 K neutron powder diffraction data (global $\chi^2 = 1.68$). This means that the oxygen diffusion is involved in phase separation phenomen. Redistribution of the oxygen ions leads to the appearance of both oxygen-rich ferromagnetic phase and oxygen-poor antiferromagnetic one. One can suggest that the real symmetry of both antiferromagnetic and ferromagnetic phase is lower than a cubic however we did not observe corresponding NPD and SPD peaks splitting.

It is worth noting that the oxygen content of the antiferromagnetic phase is close to that for the double-layered perovskite $LaBaCo_2O_{5.5}$ [20]. In this compound, La and Ba ions are ordered forming alternative layers with only one type of ions, and the oxygen vacancies are ordered as well. In accordance with NPD study [20] the magnetic structure is antiferromagnetic G-type, similarly to that of disordered $La_{0.5}Ba_{0.5}CoO_{2.75}$. However, the Neel point is much higher than that for disordered phase. The high Neel point of the ordered phase is associated with optimal geometry of negative and positive magnetic interactions. The contention between positive and negative interactions leads to stabilization of non-collinear magnetic structure and appearance of a spontaneous magnetization [19, 24]. Both $La_{0.5}Ba_{0.5}CoO_{2.75}$ and $LaBaCo_2O_{5.5}$ contain one half of Co ions in CoO_5 pyramids and another half in CoO_6 octahedra. The electron configuration of Co ions located in the pyramids agrees with the high-spin state whereas for Co ions in the octahedral sites the low-spin state seems to be dominant [25]. The calculated magnetic moment for the antiferromagnetic $La_{0.5}Ba_{0.5}CoO_{2.75}$ phase seems to agree with this suggestion. For Co^{3+} (HS) ion the expected magnetic moment value is between 3 and $4\mu_B$ [24, 25] whereas the observed one is $2.1\mu_B$, thus suggesting smaller magnetic moment in the octahedra. In layered perovskites, every Co^{3+} ion in the high-spin state interacts antiferromagnetically with three Co^{3+} (HS) and ferromagnetically with one Co^{3+} (HS) in the absence of a common oxygen bridge. There are only two Co^{3+} (LS) nearest neighbors. Another situation is realized in disordered $La_{0.5}Ba_{0.5}CoO_{2.75}$ where Co^{3+} (HS) interacts only with three Co^{3+} (HS) on average, and the positive and negative interactions are equally probable. In this case there are three Co^{3+} (LS) nearest neighbors on average. The larger concentration of the Co^{3+} (LS) nearest neighbors favors the lower Neel point in comparison with layered cobaltites. We suggest that the antiferromagnetic interactions are stronger and thus the antiferromagnetic structure is realized.

It is worth noting that the phase separation in $La_{0.5}Ba_{0.5}CoO_{2.87}$ and tetragonal distortion in stoichiometric $La_{0.5}Ba_{0.5}CoO_3$ [13] have similar temperature dependences. Both effects start to develop near the Curie point and increase gradually with cooling. Apparently magnetic interactions play important role in the observed phase separation. Another factor seems to be important for phase separation is large unit cell volume of $La_{0.5}Ba_{0.5}CoO_{2.87}$ in comparison with Sr-doped cobaltites; this favors stabilization of the Jahn-Teller-active intermediate spin state in the octahedra. The metallic-like character of the ferromagnetic phase in cobaltites should be taken into account also. The observed macroscopic phase separation in the cobaltites can be compared with macroscopic phase separation into insulating antiferromagnetic and superconducting phases in $La_2CuO_{4+\delta}$ [26, 27]. It was suggested [27] that cuprates can exhibit phase separation for two related reasons: the onset of antiferromagnetic correlations and the onset of Mott insulating gap. In $La_2CuO_{4+\delta}$ the macroscopic phase separation is made possible by the mobility of the interstitial oxygen dopants which follow the holes and maintain charge neutrality. In $La_2CuO_{4+\delta}$ the interstitial oxygen is mobile down to 170 K whereas in $La_{0.5}Ba_{0.5}CoO_{2.87}$ phase separation occurs at much lower temperatures due to very large mobility of the oxygen vacancies in cobaltites. The nanoscale phase separation into ferromagnetic and paramagnetic clusters have been observed in the lightly doped cobaltites [28]. However these compounds are stoichiometric, so macroscopic phase separation is not realized.

In conclusion, high-resolution neutron and synchrotron powder diffraction studies of the non-

stoichiometric compound $La_{0.5}Ba_{0.5}CoO_{2.87}$ revealed the macroscopic structural phase separation into oxygen poor antiferromagnetic and oxygen-rich ferromagnetic phases which starts to develop slightly above a transition into a magnetically ordered state. Both antiferromagnetic and ferromagnetic phases have a crystal structure very close to cubic. The amount of antiferromagnetic phase increases gradually with cooling, and the calculated ratio between antiferromagnetic and ferromagnetic phases at 2 K is about 1:2. The calculated magnetic moment is $\pm 2.1\ \mu_B$/Co for the antiferromagnetic and $1.6\,\mu_B$/Co for the ferromagnetic phase.

This work was supported by Belarussian Fund for Fundamental Research (grant # F09F-003).

1. J. B. Goodenough and J. S. Zhou, *Structure and bonding*, Ed. J.B. Goodenough, Springer, New York, 2001
2. A. Podlesnyak, S. Streule, J. Mesot et al., Phys. Rev. Lett. **97**, 247208 (2006).
3. M. W. Haverkort, Z. Hu, J. C. Cezar et al., Phys. Rev. Lett. **97**, 176405 (2006).
4. D. P. Kozlenko, N. O. Golosova, Z. Jirak et. al., Phys. Rev. B **75**, 064422 (2007).
5. R. F. Klie, J. C. Zheng, Y. Zhu et al., Phys. Rev. Lett. **99**, 047203 (2007).
6. J. Wu and C. Leighton, Phys. Rev. B **67**, 174408 (2003).
7. P. Mandal, P. Choudhury, S. K. Biswas et al., Phys. Rev. B **70**, 104407 (2004).
8. M. Kriener, C. Zobel, A. Reichl et al., Phys. Rev. B **69**, 094417 (2004).
9. A. P. Sazonov, I. O. Troyanchuk, H. Gamari-Seale et al., J. Phys.: Condens. Matter **21**, 156004 (2009).
10. J. B. Goodenough, Mater. Res. Bull. **6**, 967 (1971).
11. M. Senaris-Rodriguez and J. Goodenough, J. Solid State Chem. **118**, 323 (1995).
12. D. Louca, J. L. Sarrao, J. D. Thompson et al., Phys. Rev. B **60**, 10378 (1999).
13. F. Fauth, E. Suard, and V. Caignaert, Phys. Rev. B **65**, 060401(R) (2001).
14. V. Sikolenko, A. Sazonov, I. Troyanchuk et al., J. Phys.: Condens. Matter **16**, 7317 (2004).
15. V. Sikolenko, V. Efimov, E. Efimova et al., J. Phys.: Condens. Matter **221**, 436002 (2009).
16. N. Sundaram, Y. Jiang, I. E. Anderson et al., Phys. Rev. Lett. **102**, 026401 (2009).
17. I. O. Troyanchuk, N. V. Kasper, D. D. Khalyavin et al., Phys. Rev. Lett. **80**, 3380 (1998).
18. A. Maignan, C. Martin, D. Pelloquin et al., J. Solid State Chem. **142**, 247 (1999).
19. M. Soda, Y. Yasui, M. Ito et al., J. Phys. Soc. Japan **73**, 464 (2004).
20. E. L. Rautama, V. Caignaert, Ph. Boullay et al., Chem. Mater. **21**, 102 (2009).
21. Z. L. Wang and J. S. Yin, Philosophical Magazine Part B **77**, 49 (1998).
22. J. Rodriguez-Carvajal, Physica B **192**, 55 (1993).
23. D. N. H. Nam, K. Jonason, P. Nordblad et al., Phys. Rev. B **59**, 4189 (1999).
24. I. O. Troyanchuk, D. V. Karpinsky, and F. Yokachiya, J. Phys.: Condens. Matter **20**, 335228 (2008).
25. M. Soda, Y. Yasui, Y. Kobayashi et al., J. Phys. Soc. Japan **75**, 104708 (2006).
26. P. G. Radaelli, J. D. Jorgensen, R. Kleb et al., Phys. Rev. B **49**, 6239 (1994).
27. B. V. Fine and T. Egami, Phys. Rev. B **77**, 014519 (2008).
28. J. Wu, J. W. Lynn, C. J. Glinka et al., Phys. Rev. Lett. **94**, 37201 (2005).